

# Polarization effects in $K^+$ – $Na^+$ ion exchanged MMI structures with absorption cover

ARTUR SZEWCZUK\*, MAREK BŁAHUT

Department of Optoelectronics, Silesian University of Technology,  
ul. Bolesława Krzywoustego 2, 44-100 Gliwice, Poland

\*Corresponding author: artur.szewczuk@polsl.pl

The paper concerns the polarization effects in gradient index MMI sensor structures made by ion  $K^+$ – $Na^+$  exchange. It has been shown both experimentally and based on the numerical calculation that for the  $K^+$ – $Na^+$  ion exchanged MMI structures, propagation conditions of light in multimode section vary considerably for each polarization. There are presented the possibilities of using this effect in application to gas sensing. Analyzed sensor structures are covered by  $WO_3$  absorbing nanolayers. Numerical analyses of MMI sensor are performed and modal attenuation coefficients are determined. The comparison between operation characteristics obtained for the TE and TM polarization is presented.

Keywords: multimode interference, optical sensors, modal attenuation.

## 1. Introduction

Multimode interference structures due to their properties are interesting objects of research. The basis of these structures is the phenomenon of input field imaging for the certain propagation length. This characteristic property of these structures can be used in many different ways. The most popular is the use of these optical elements as waveguide splitters [1]. Among many other applications there is also described the scientific work on the use of MMI structures as optical sensors [2–4]. The operation principle of each of these devices described in many scientific publications is similar. In most cases, the multimode section is covered with a layer whose optical parameters are changed when exposed to a measured medium. The changes in external physical parameters lead to the changes in propagation conditions of light, and this effect is easily observable in the output signal. The paper [2] proposes an optical temperature sensor based on MMI structures in silicon. Temperature changes cause changes in the refractive index of the interference section. The studies [3, 4] apply to interference structures made in planar waveguides by a sol–gel method and describe technological and experimental research of a water vapour sensor and numerical simulation of the optical system of the interference gas sensor.

This problem was also considered by the authors of this study in the Refs. [5–7], in which we analyzed the possibility to use multimode interference phenomena in waveguide sensors. The aim of this study is to examine the possibility of using polarization effects occurring in ion exchanged waveguides, in optical sensors technology. The investigated gradient index MMI structures are produced in the  $K^+Na^+$  ion exchange process. Investigation was carried out for both polarizations TE and TM. This distinction into two polarizations is necessary since for the gradient index MMI structures produced in the  $K^+Na^+$  ion exchange process, propagation conditions of light are different for each polarization [8]. As shown in this work, operation characteristics of a refractometer based on such structures vary considerably.

## 2. Optical structures configurations

Multimode interference structures consist of three sets of waveguides: single-mode input and output waveguides and multimode section placed between them. When exciting a multimode waveguide, we can observe the matching of input field to the modal fields of the waveguide, and then the interference of the excited waves. In effect of the intermodal interference, a so-called self-imaging of the input field is taking place. As a result of this effect, the input field is reproduced in simple, reflected and multiple images [1].

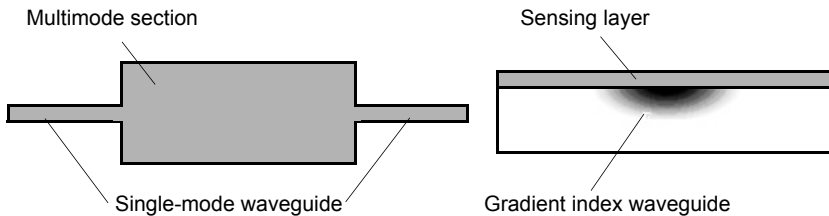


Fig. 1. Model of MMI sensor.

The basis of the research described in this paper is a gradient index MMI structure (Fig. 1) with multimode section length relating to the length of the input field image formation. Multimode section is covered with material which changes its optical parameters (refractive index and extinction coefficient) when exposed to appropriate gaseous environments. The coating parameters changes have an effect on light propagation condition in structure and can be seen as the output signal variation. In this configuration, there are several factors responsible for changes in the registered output signal. Variations of a coating layer refractive index influence the mode properties of the multimode waveguide, which results in the input field image position and the output signal value. In the case of the absorption layer, the refractive index changes have also influenced the modal attenuation value by changing the shape of the modal field distribution, which leads to a reduction or increase in the amount of light penetrating the absorbing sensing layer. This effect is different for different modes. Depending on the properties of a sensor layer – its refractive index and

extinction coefficient – there is observed the predominance of the first (phase) or second (absorbing) effect. In this paper, we focus on the absorbing effect occurring in the metal oxides sensing layers used to measure the gas concentrations.

### 3. Waveguide materials properties

#### 3.1. Gradient index core

The investigated MMI sections are produced in the  $K^+Na^+$  ion exchange process in the time of 0.75 h and temperature of 400 °C in borosilicate glass. The distribution profile of a refractive index of MMI section obtained in the diffusion process is calculated numerically from the nonlinear diffusion equation [7–9]:

$$\frac{\partial C_K}{\partial t} = \nabla \left[ \frac{D_K}{1 - (1 - m)C_K} \nabla C_K \right] \quad (1)$$

where  $C_K$  is the dopant  $K^+$  ions concentration, proportional to the refractive index change. Material parameters of the technological process – self-diffusion coefficient of  $K^+$  ions  $D_K$ , the mobility ratio  $m$  of the ions  $K^+$  and  $Na^+$ , and the maximum of the refractive index change – were determined by measurements of respective planar index profiles using the IWKB method [8].

The determined self-diffusion coefficient is equal to  $2.18 \mu\text{m}^2/\text{h}$  for both profiles, whereas the distribution maxima on the surface are equal to respectively 0.0095 and 0.0117. The observed differences in the distribution of the refractive index for both orthogonal polarizations (Fig. 2) result from the anisotropy of strains taking place during the technological process, and are of significant importance for performance characteristics of the MMI.

Birefringence of these waveguides manifests itself in different modal fields distributions and in particular in the different input field image position. Furthermore,

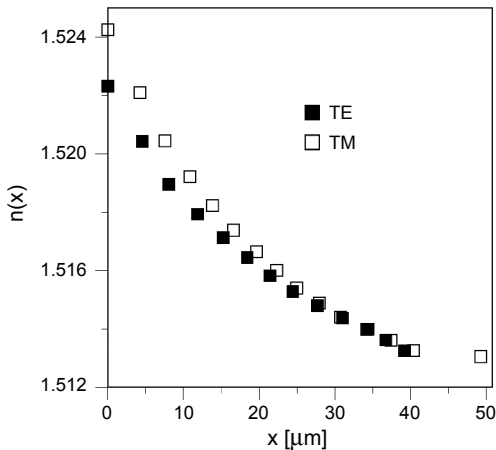
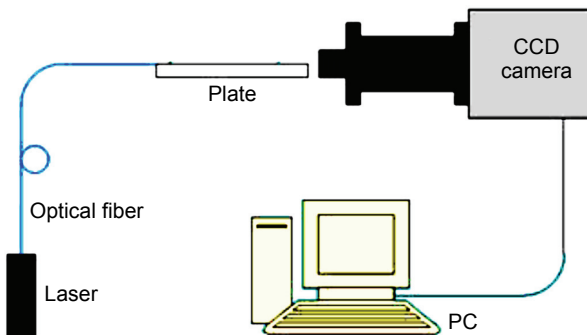


Fig. 2. Profiles of refractive index for TE and TM waves in BK-7 glass.

the wave of TE and TM polarization will react differently with the sensing layer. This will result in different operating characteristics for each polarization. Polarization effects in birefringent MMI structures obtained by the ion exchange process were discussed in detail by the author in the paper [8].

The differences in field distributions for each polarization can be easily shown during the output signal registration of the  $1 \times N$  splitter based on multimode interference structures made with ion-exchange technology. These optical elements consist of multimode section of a length corresponding to the formation of  $N$ -fold input field image and output single-mode waveguides placed at the output of the MMI section in the place, where the input field is reproduced. In this way, a uniform distribution of the signal is obtained. The splitter basing on birefringent waveguides can work properly only for one polarization, for which the dimensions have been optimized. In the case of optical sensor based on MMI structures, polarization changes will affect the position of the operating point.

MMI structures were analyzed on the test bench as shown in Fig. 3. The MMI section in which the mode field's interference is observed was excited from a laser by the light of wavelength  $\lambda = 0.63 \mu\text{m}$ . Registration was carried out using a CCD camera with an optical system that provides high magnification. The optical system contained a Wollaston prism, which allowed observation of both polarizations simultaneously. Length of multimode section has been chosen to receive  $N$ -fold input field image for the TE polarization at the end of the section. The output signals are registered by single-mode output waveguides. MMI structures with divided signals in different ways  $1 \times 2$ ,



◀ Fig. 3. The experimental stand.

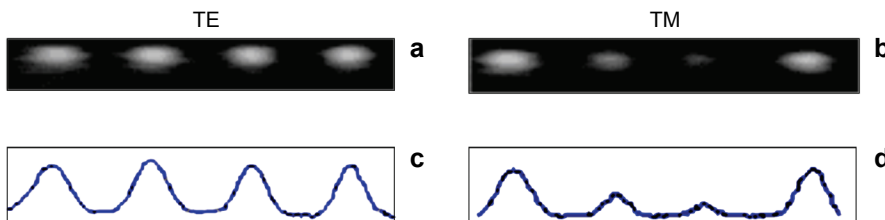


Fig. 4. The output signal; TE modes (a), TM modes (b), cross-section of registered signal (c and d).

$1 \times 3$ ,  $1 \times 4$  were studied. For example, an image obtained for  $1 \times 4$  splitter was presented in Fig. 4.

Widths of the masks of MMI section and the single-mode waveguide are 60 and 5  $\mu\text{m}$ , respectively. The output signal recorded by the CCD camera is presented in Figs. 4a and 4c. There are presented the cross-sections of registered signals.

For the TE polarization, light in each waveguide propagates with the same intensity. The situation is different for the TM polarization. For this polarization, MMI section length does not guarantee the uniform  $N$ -fold image formation of the input field (Figs. 4c and 4d). This demonstrates that lengths of  $N$ -fold images for MMI sections produced in the  $K^+Na^+$  ion exchange process depend on the polarization of guided light.

### 3.2. Sensing layer

For the analyzed concept, we have modelled a sensor layer making use of the parameters of the  $WO_3$  material, being a popular sensor material applied in gas sensors. Refractive index and extinction coefficient values needed for calculations are approximated on the basis of experimental values shown in [10] (Fig. 5) as a function of volumetric density of absorbed charge which is proportional to the gas concentration.

## 4. Numerical analysis of the impact of MMI section cladding parameters on the signal transmission for TE and TM modes

### 4.1. Modal attenuation

The evanescent field of modes propagating in multimode waveguide penetrates the absorbing sensor layer. Due to a relatively high value of the sensor layer extinction coefficient, light can be strongly attenuated just at short propagation distance [5, 11]. To determine modal attenuation coefficients we transform 2-D problem to 1-D using

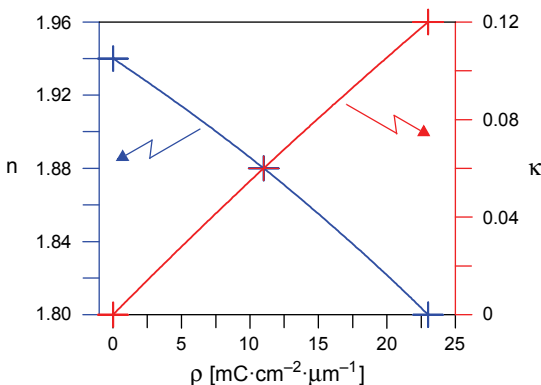


Fig. 5. Optical parameters of  $WO_3$  layers [11].

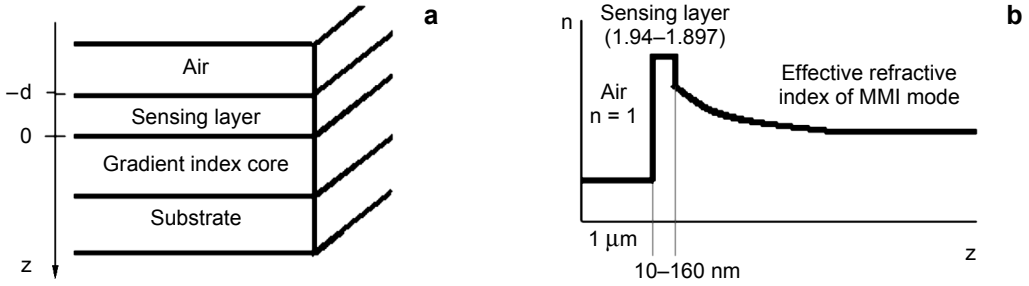


Fig. 6. Configuration of optical structure: layers configuration (a), refractive index profile (b).

the effective index method. The analyzed 1-D layer structure is shown in Fig. 6. The refractive index profile of the analyzed structure for equivalent refractive index distributions, obtained for each  $[0, n]$  mode of MMI structure by the effective index method is presented in Fig. 6b.

The formula on the modal attenuation coefficient  $\gamma_m^{\text{TE}}$  of TE modes of the order  $m$  can be expressed by the equation [12]:

$$\gamma_m^{\text{TE}} = \frac{2k_0 n \kappa}{N_m^{\text{TE}}} \frac{\int_{-d}^0 E_y^2 dz}{\int_{-\infty}^{\infty} E_y^2 dz} \quad (2)$$

For TM modes, the following is obtained respectively:

$$\gamma_m^{\text{TM}} = \frac{2k_0 n \kappa}{N_m^{\text{TE}}} \left[ 2 \left( \frac{N_m^{\text{TM}}}{n} \right)^2 - 1 \right] \frac{\int_{-d}^0 \frac{1}{n(r)^2} H_y^2 dz}{\int_{-\infty}^{\infty} \frac{1}{n(r)^2} H_y^2 dz} \quad (3)$$

where  $k_0$  denotes the wave vector in vacuum,  $n$  and  $\kappa$  are respectively the refractive index and the extinction coefficient of the sensor layer,  $d$  denotes the sensor layer thickness,  $N_m^{\text{TE}}$  and  $N_m^{\text{TM}}$  are the effective indices of TE and TM mode of order  $m$ ;  $E$  and  $H$  are respectively the value of electric and magnetic fields.

The larger part of the mode field propagates in cover, the greater is the value of its attenuation coefficient. Figure 7a shows for instance the calculated wave function distributions in the direction perpendicular to the substrate of TE mode propagating in multimode structure of the width of 30  $\mu\text{m}$ . MMI structures are covered by the sensor layer of the refractive index of 1.94 and different layer thicknesses. The analogous characteristics for TM modes are presented in Fig. 7b.

The modal attenuation is low for very thin sensing layers (Fig. 8). In this case, the mode energy is guided mainly in the core and its evanescent part is very small. Together with the increase in the layer thickness also the part of the mode field which penetrates the cover, increases and the attenuation rapidly grows. For the suitable large thicknesses of the cover, the first order mode appears. The attenuation coefficient of

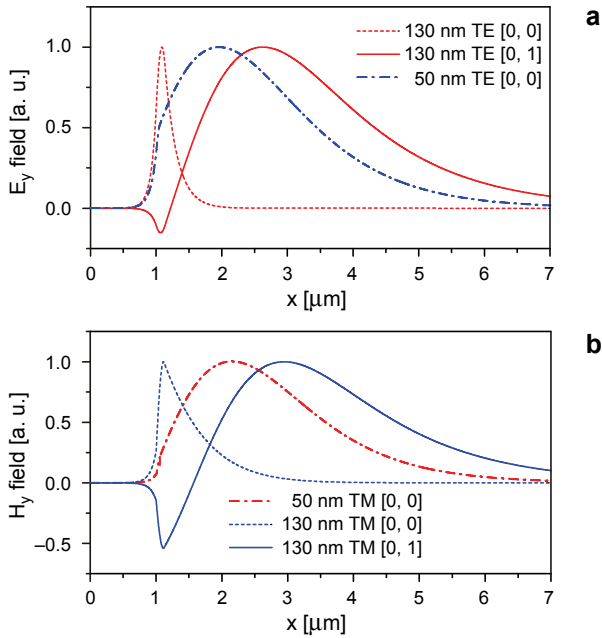


Fig. 7. Modal field distributions of analyzed waveguide structures for the MMI section width of  $30\ \mu\text{m}$  and different sensor layer thicknesses for TE (a) and TM (b) modes.

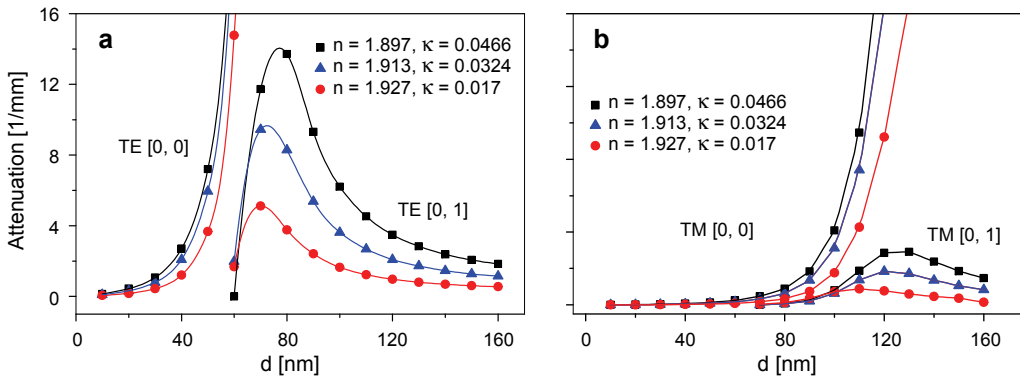


Fig. 8. Attenuation coefficient of the core mode in MMI structure as a function of sensor layer thickness for different refractive index  $n$  and extinction coefficient  $\kappa$  of the layer for TE (a) and TM (b) modes.

this mode increases together with the layer thickness reaching the maximum value, then the evanescent part of the field in the cover decreases and attenuation also decreases.

Comparison of the characteristics obtained for the modal attenuation shows that the value of the TM modes attenuation increases much more slowly with increasing thickness of the cover than in the case of the TE modes. Optical power densities of TM modes are not smooth at the layers borders as distinguished from TE modes. This

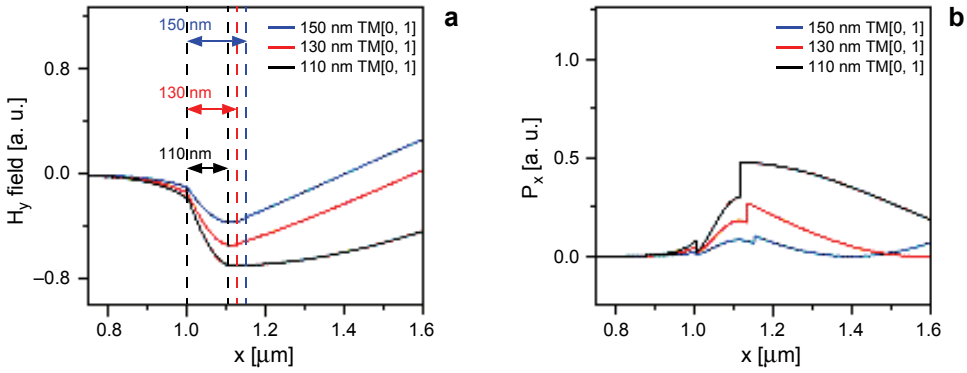


Fig. 9. Modal field distribution (a) and Poynting vector component in the direction of propagation  $P_x$  (b) in absorbing layer for TM [0, 1] modes.

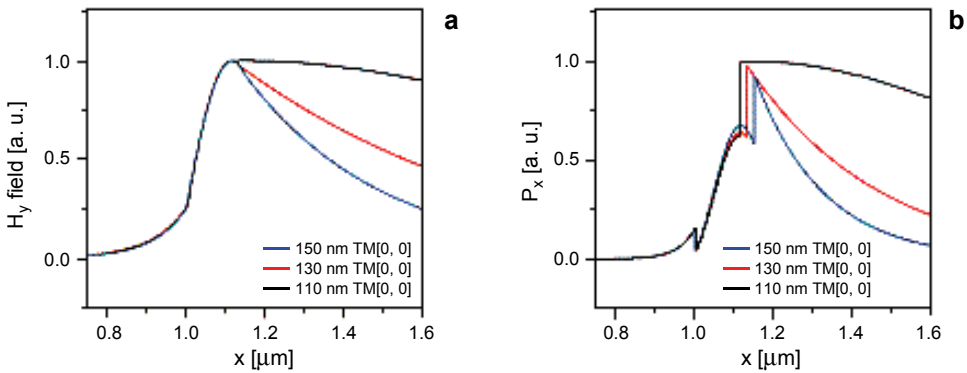


Fig. 10. Modal field distribution (a) and Poynting vector component in the direction of propagation  $P_x$  (b) in absorbing layer for TM [0, 0] modes.

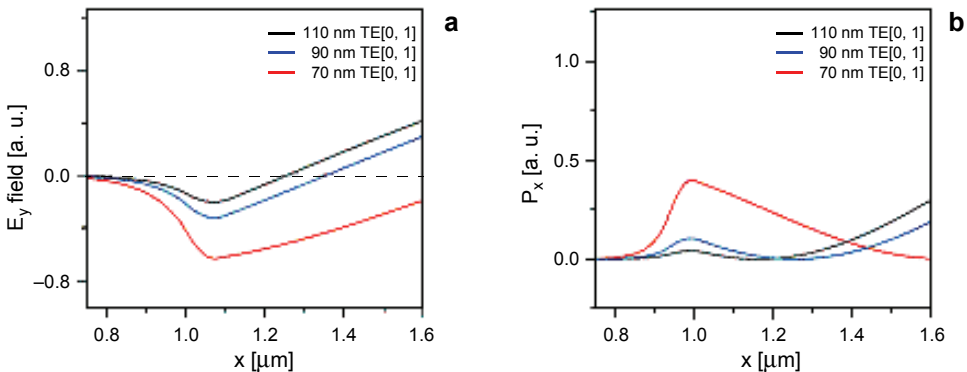


Fig. 11. Modal field distribution (a) and Poynting vector component in the direction of propagation  $P_x$  (b) in absorbing layer for TE [0, 1] modes.



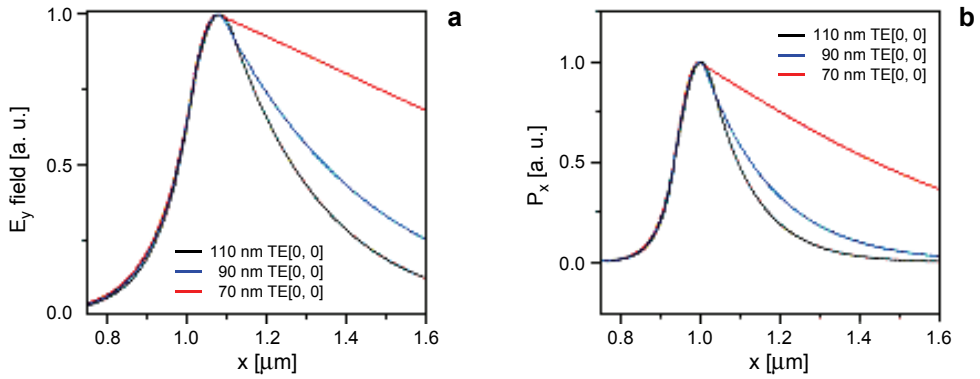


Fig. 12. Modal field distribution (a) and Poynting vector component in the direction of propagation  $P_x$  (b) in absorbing layer for TE [0, 0] modes.

manifests itself in a stepwise decreasing value of the Poynting vector component in the direction of propagation in a sensing layer (Figs. 9 and 10). In such a case, an increase in the layer thickness has not a significant impact on an increase in the attenuation coefficient as it is in the case of the TE polarization (Figs. 11 and 12).

The number of propagating modes in the multimode section is dependent on the width of the section. Each of these modes is characterized by a different value

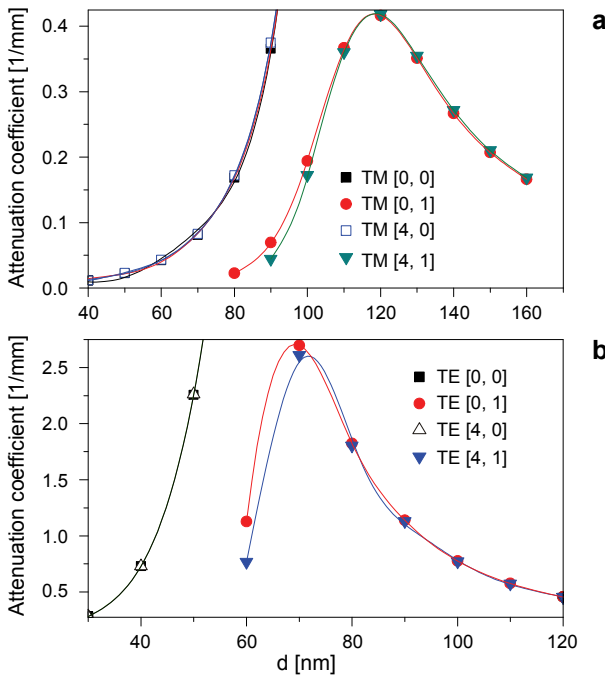


Fig. 13. Attenuation coefficient of mode in MMI structure as a function of sensor layer thickness for different order number TM (a) and TE (b) modes.

of the attenuation coefficient. Figure 13a shows the dependence of modal attenuation for TM  $[0, 0]$ ,  $[0, 1]$ ,  $[4, 0]$  and  $[4, 1]$  modes. Calculations were carried out for  $70 \mu\text{m}$  waveguides width, covered refractive index 1.934 and extinction coefficient 0.00878. In the case of TM modes  $[n, 0]$ , the attenuation values of each modes are on the same level. More noticeable differences occur in the case of TM modes  $[n, 1]$  for the appropriate thickness of a sensor. In this case, there is a possibility to select the configuration for which a lower order mode will be stronger attenuated, and the signal will be transmitted only by high order modes with lower attenuation. A similar characteristics were made for TE polarization (Fig. 13b).

The offset of the two characteristics obtained for TE and TM polarization is clearly visible. The first order mode for TM polarization appears for the thicker coating layer than it is in the case of TE polarization. This is due to the different refractive index profile corresponding to each polarization. TE polarization is characterized by a higher effective refractive index which determines that conditions for the excitation of a next order mode are met for a thinner cover than it is in the case of TM modes.

## 4.2. Operation characteristics of MMI sensor

Changes in the refractive index and extinction coefficient of the sensing layer have an impact on the mode properties of multimode waveguides, as a result influencing the location of the input field image. Attenuation in the sensitive layer decreases

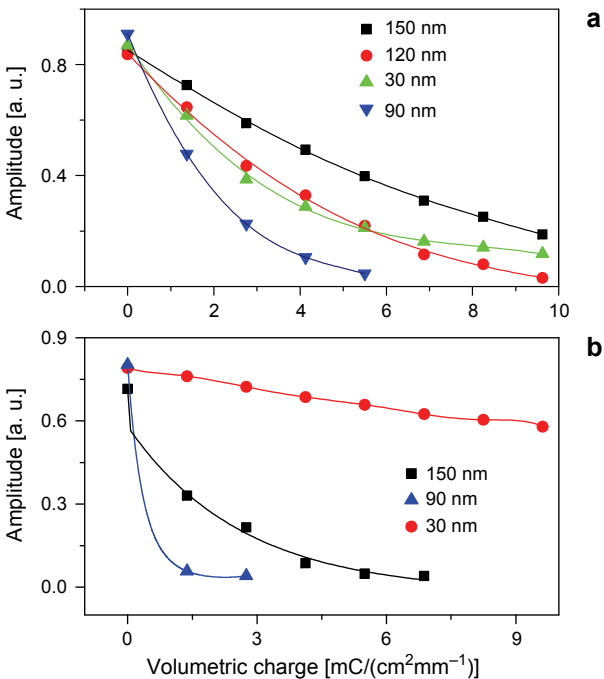


Fig. 14. Output field amplitude as a function of the optical and geometrical parameters of the sensing layer for different sensing layer thicknesses for TE (a) and TM (b) polarization.

additionally the signal level. The output signal changes are registered by a single-mode output waveguide.

Taking into consideration the results of mode attenuation, the operation characteristics of MMI sensor are made using the beam propagation method (BPM) for different thicknesses of sensor layers for both polarizations.

Calculations are carried out for MMI section of the width of 30  $\mu\text{m}$ . Its length, selected to obtain the 1-fold image for TE polarization of the input field, amounts to 2300  $\mu\text{m}$  for the refractive index of the cover equal to 1.94. This value of the refractive index and the value of extinction coefficient equal to zero, are the layers parameters which fix the operation point of the sensor. Figures 14a and 14b present the output field amplitude as a function of absorbed volumetric charge in the sensor layer for different values of the layer thicknesses for the TE and TM modes, respectively.  $\text{WO}_3$  layer optical parameters as a function of absorbed volumetric charge are taken from Fig. 5.

## 5. Conclusions

Thickness of the sensing layer is the key parameter which affects the operation characteristics of an optical sensor with a high refractive index absorption cover. For a given thickness, operation characteristics for each polarization vary considerably. This enables to design such a sensor configuration that can operate simultaneously on narrow and wide range of cover parameters changes. In one mode of operation, it would be possible to work in a selected narrow range of sensing layer parameters changes with high sensitivity. At the same time it would be possible for the second polarization to obtain information about cover parameters changes of a wider range, but with less sensitivity.

*Acknowledgements* – The work was sponsored by the State Committee for Scientific Research (NCBiR) within the grant N R01 034 06/2009. Author (AS) received the grant under the project DoktorIS – Scholarship program for innovative Silesia co-financed by the European Union under the European Social Fund.

## Reference

- [1] BŁAHUT M., KASPRZAK D., *Multimode interference structures – properties and applications*, *Optica Applicata* **34**(4), 2004, pp. 573–587.
- [2] IRACE A., BREGGIO G., *All-silicon optical temperature sensor based on multi-mode interference*, *Optics Express* **11**(22), 2003, pp. 2807–2812.
- [3] KRIBICH K.R., COPPERWHITE R., BARRY H., KOŁODZIEJCZYK B., SABATTIÉ J.-M., O'DWYER K., MACCRAITH B.D., *Novel chemical sensor/biosensor platform based on optical multimode interference (MMI) couplers*, *Sensors and Actuators B* **107**(1), 2005, pp. 188–192.
- [4] MAZINGUE T., KRIBICH R.K., ETIENNE P., MOREAU Y., *Simulations of refractive index variation in a multimode interference coupler: Application to gas sensing*, *Optics Communications* **278**(2), 2007, pp. 312–316.
- [5] SZEWCZUK A., BŁAHUT M., *Multimode interference structures of variable geometry for optical sensor application*, *Acta Physica Polonica A* **118**(6), 2010, pp. 1254–1258.

- [6] SZEWCZUK A., BŁAHUT M., PYKA W., *Model of optical sensor on the base of MMI structures*, Acta Physica Polonica A **118**(6), 2010, pp. 1250–1253.
- [7] SZEWCZUK A., BŁAHUT M., *Applications of gradient index multimode interference structures in the technology of optical sensor*, Acta Physica Polonica A **120**(4), 2011, pp. 740–743.
- [8] KASPRZAK D., BŁAHUT M., *Polarization effects in gradient index MMI structures made by  $K^+ \leftrightarrow Na^+$  ion exchange*, Proceedings of the 14th European Conference on Integrated Optics ECIO 2007, April 25–27, 2007, Copenhagen, Denmark, p. THG15.
- [9] KARASIŃSKI P., *Influence of waveguide parameters on the difference interference in optical planar structure*, Optica Applicata **32**(4), 2002, pp. 775–796.
- [10] VON ROTTKAY K., RUBIN M., WEN S.-J., *Optical indices of electrochromic tungsten oxide*, Thin Solid Films **306**(1), 1997, pp. 10–16.
- [11] GUT K., PUSTELNY T., *Attenuation planar waveguides with an absorbing cover*, Journal de Physique IV **129**, 2005, pp. 113–116.
- [12] KARASIŃSKI P., ROGOZIŃSKI R., *Influence of refractive profile shape on the distribution of modal attenuation in planar structures with absorption cover*, Optics Communications **269**(1), 2007, pp. 76–88.

*Received October 10, 2012  
in revised form March 13, 2013*